

Graphene Oxide: A Convenient Metal-Free Carbocatalyst for Facilitating Aerobic Oxidation of 5-Hydroxymethylfurfural into 2,5-Diformylfuran

Guangqiang Lv,^{†,‡} Hongliang Wang,[†] Yongxing Yang,[†] Tiansheng Deng,[†] Chengmeng Chen,[§] Yulei Zhu,^{||} and Xianglin Hou^{*,†}

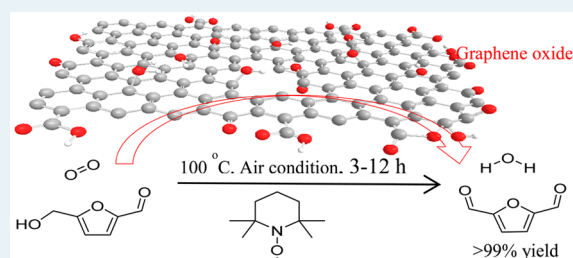
[†]The Biorefinery Research and Engineering Center, [§]Key Laboratory of Carbon Materials, ^{||}State Key Laboratory of Coal Conversion, Institute of Coal Chemistry, Chinese Academy of Sciences, 27 South Taoyuan Road, Taiyuan 030001, People's Republic of China

[‡]University of Chinese Academy of Sciences, Beijing 100039, People's Republic of China

Supporting Information

ABSTRACT: By thermal treatment in vacuum, graphite oxide prepared by Hummer's method was exfoliated and partially reduced. This procedure imparts to the graphene oxide (GO) high reactivity with 2,2,6,6-tetramethylpiperidin-1-oxyl (TEMPO) as cocatalyst for selective oxidation of 5-hydroxymethylfurfural (HMF) to 2,5-diformylfuran (DFF) under certain conditions (100% HMF conversion with HMF selectivity 99.6% at 80 wt % GO loading, 1 atm air pressure). This study found that GO could function as an oxidant for anaerobic oxidation of HMF during which carboxyl groups in GO were reduced. Importantly, the partially reduced GO material could continue to activate molecular oxygen during aerobic oxidation. Further study showed that oxygen functionalities in the GO material had a crucial effect on the catalytic oxidation of HMF. By control experiments and molecular analogues tests, a plausible mechanism was proposed in which the high reactivity was attributed to the synergistic effect of the carboxylic acid groups and unpaired electrons at GO edge defects, with TEMPO as the cocatalyst and oxygen as the terminal oxidant.

KEYWORDS: graphene oxide, metal-free carbon catalyst, selective oxidation, 5-hydroxymethylfurfural, 2,5-diformylfuran



INTRODUCTION

Rapidly depleting fossil fuels and escalating energy consumption coupled with rising environmental awareness among nations have led to an increased focus on alternative, viable, ecofriendly, and renewable energy sources. Biomass is becoming more attractive as a logical alternative to petroleum because it is the only available carbon source apart from fossil resources.¹

5-Hydroxymethylfurfural (HMF), which is a dehydration product of C₆-based carbohydrates, has been regarded as one of the most promising platform chemicals and can be used as a versatile precursor for the production of fine chemicals, plastics, pharmaceuticals, and liquid fuels. Selective oxidation of HMF is one of the most pivotal transformations in biorefinery.² 2,5-Diformylfuran (DFF), as an oxidation product of HMF, can be used for the synthesis of furan-containing polymers and materials with special properties. It can also be used as a starting material for the synthesis of various poly-Schiff bases, pharmaceuticals, antifungal agents, organic conductors, and cross-linking agents of poly(vinyl alcohol) for battery separations.³ In early reports, DFF has primarily been synthesized from the oxidation of HMF by use of stoichiometric oxidants, including NaOCl,⁴ BaMnO₄,⁵ and pyridinium chlorochromate.⁶ These methods not only consumed stoichiometric oxidant but also produced large amounts

of waste. In recent years, there has been growing attention on the synthesis of DFF from HMF oxidation with molecular oxygen as the terminal oxidant catalyzed by heterogeneous or homogeneous metal catalysts such as Co/Ce/Ru,¹ Ru,^{1,7,8} Cu,⁹ Cu/V,¹⁰ Mn,¹¹ Mo/V,¹² and V.^{13,14} These catalysts often give a relatively high yield of DFF; however, the transition-metal-based catalysts applied in oxidative transformation are usually expensive, toxic, and difficult to remove.¹⁵

Graphene oxide (GO), a readily available and inexpensive material, historically has functioned primarily as a precursor to reduced graphene oxide (rGO) or chemically modified graphene (CMG) materials.^{16,17} GO-related materials have generated tremendous excitement owing to their remarkable electronic, mechanical, and chemical properties.^{18–22} The relatively harsh conditions used in typical GO synthetic protocols (Hummer's method) have introduced a variety of oxygen-containing functionalities (e.g., hydroxyl, epoxide, carboxylic acids, ketones, phenols, lactols, and lactones).²³ As a result, these functionalities make GO slightly acidic (pH 4.5 at 0.1 mg mL⁻¹) and endow it with rather strong oxidizing properties.²⁴

Received: April 8, 2015

Revised: August 9, 2015

Published: August 21, 2015

To date, GO or rGO has been utilized as a catalyst support,^{25–27} solid acid,²⁸ oxidant,^{15,29} chemically modified graphene (CMG) carbocatalyst used in the oxygen reduction reaction,^{30–33} and acetylene and alkene hydrogenation.³⁴ It is believed that GO doping is a powerful strategy to modulate the electronic structure of sp^2 carbon material and introduce catalytically relevant active sites. N-doped graphene and active carbon have been successfully employed in aerobic oxidation of benzylic alcohols, hydroxyl alcohol, and HMF.^{35,36} N-doped and N–S-doped graphene show high efficiency in the *trans*-stilbene epoxidation reaction³⁷ and catalytic oxidation of phenol.³⁸ Recently, Dreyer et al reported GO could be used as a metal-free carbocatalyst to selectively oxidize benzyl alcohol to benzaldehyde with high selectivity using molecular oxygen as the terminal oxidant.¹⁵ Su et al.³⁹ reported the oxidative coupling of amines into imines with base- and-acid processed GO material as the metal-free catalyst. In this paper, we report GO can be used as an efficient carbocatalyst for selective oxidation of HMF into DFF with full conversion and nearly 100% selectivity under optimized conditions. By XPS tests and other control experiments, we have identified that the lattice oxygen species in the form of carboxylic acids are responsible for the oxidation reaction.

RESULTS AND DISCUSSION

Synthesis of GO Nanosheets. The GO materials used in this investigation were prepared by thermal exfoliation of graphite oxide, which was prepared by oxidation of graphite by a modified Hummers' method, at 200 °C under vacuum (25 Torr). The details of the synthesis are described in the [Supporting Information](#). The specific surface area was determined by N_2 adsorption/desorption analysis and calculated by the Brunauer–Emmett–Teller (BET) model (Figure 1a). The obtained GO material has a BET surface area of 340.6 m^2/g with an average pore diameter of 14.3 nm.

Figure 1b shows the XRD profiles of the graphite oxide and thermal exfoliated GO. Graphite oxide represents one main reflection centered at 10.9° , corresponding to a *c*-axis interlayer spacing of 0.81 nm. It indicates that graphite is oxidized completely. The GO shows a weak diffraction peak at $\sim 8.6^\circ$ ($d = 1.02$ nm) and a broad diffraction peak at $\sim 28.8^\circ$ (0.32 nm), followed by the complete disappearance of the characteristic peak of GO at $\sim 10.9^\circ$. This suggests that graphite oxide have been exfoliated completely but not uniformly under these conditions.

Catalytic Test of GO in Selective Oxidation of HMF into DFF. In a preliminary experiment, 1 M mol quantity of HMF dissolved in 30 mL of acetonitrile was heated to 100 °C in the presence of 100 mg GO for 12 h under 1 atm air pressure in a 100 mL autoclave. However, subsequent analysis of the products showed that only 9.5% HMF conversion could be reached (Table 1, entry 1). The rather poor conversion compared with benzyl alcohol oxidation to benzaldehyde¹⁵ can be attributed to the low reactivity of HMF. 2,2,6,6-Tetramethylpiperidin-1-oxyl (TEMPO) has always been used as the cocatalyst for the generation of aldehydes or ketones from alcohols. CuCl/TEMPO/NCPs catalytic system was successfully applied in the oxidation of HMF into DFF.⁹ When TEMPO, which alone is not active as a catalyst or oxidant in HMF transformation (Table 1, entry 2), was introduced into this catalysis system, HMF conversion increased significantly to 89.4%, with DFF selectivity up to 98.8% (Table 1, entry 6). Increasing the amount of GO (Table

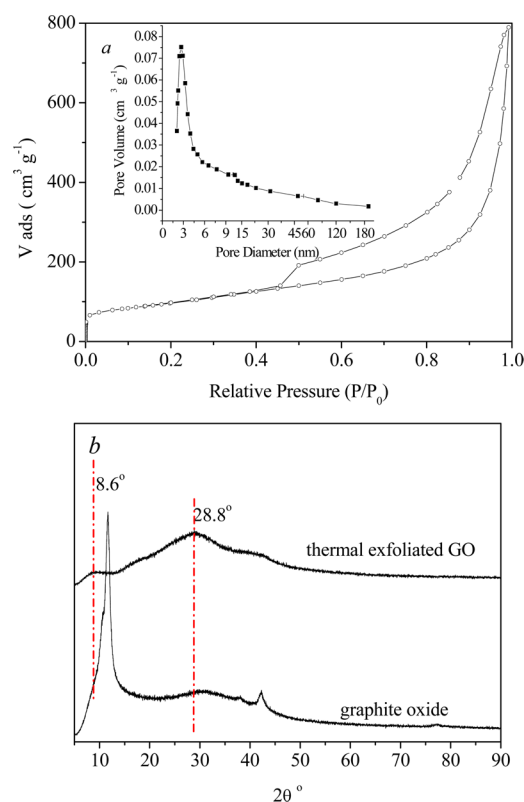


Figure 1. (a) N_2 sorption and pore size distribution of GO (b) XRD patterns of graphite oxide and thermal exfoliated GO.

Table 1. Oxidation of HMF into DFF over GO under Different Conditions^a

entry	reaction time (h)	temp (°C)	GO loading (mg)	HMF conversion (%)	DFF selectivity (%)
1 ^b	12	100	100	9.5	86.3
2	12	100	0	4.1	75.6
3	12	100	50	67.4	98.4
4	12	100	80	81.5	98.4
5	12	80	100	82.5	98.6
6	12	100	100	89.4	98.8
7	18	100	100	100	99.6
8	3	120	100	88.6	98.8
9	6	120	100	98.2	99.5
10	3	100	100	50.1	84.8
11 ^c	3	100	100	35.6	98.0
12 ^d	3	100	100	91.9	98.5
13 ^d	6	100	100	98.1	99.6
14 ^d	9	100	100	100	99.5
15 ^e	12	100	100	13.1	79.2
16 ^f	12	100	100	35.6	96.9

^aReaction conditions: HMF (1 mmol, 126 mg), acetonitrile (30 mL), TEMPO (1 mmol, 155 mg), 1 atm air pressure in 100 mL autoclave; stirring speed, 800 rpm. ^bWithout the addition of TEMPO. ^cThe air in the autoclave was removed by N_2 for 30 min before the reaction started. ^d0.4 MPa O_2 . ^eUltrasonic exfoliated GO was used as the catalyst. ^fUltrasonic exfoliated GO was treated with NaOH and HCl aqueous solution sequentially.

1, entries 3, 4, 6) or reaction temperature (Table 1, entries 5, 6, 8) is beneficial to oxidation reaction without obvious DFF selectivity loss.

To determine whether the GO was directly oxidizing HMF or functioning as a catalyst with ambient oxygen as the terminal oxidant, the aforementioned oxidation reaction was performed under an atmosphere of nitrogen. After 3 h at 100 °C, conversion of 35.6% for HMF was reached (Table 1, entry 11). Continued heating of this reaction mixture under nitrogen atmosphere afforded 98% conversion of HMF after another 21 h (Supporting Information, Table S1). In addition, although the residual catalyst was separated from the reaction mixture and reused under nitrogen atmosphere, a HMF conversion of 70% could still be reached in each cycle in 24 h and 100 °C while GO was reused for up to 8 cycles. After that, HMF conversion decreased sharply to ~40–50% in the 9–10th cycles (Supporting Information, Table S1). The obvious decrease in activity in HMF transformation can be attributed to the ability loss of GO as a direct oxidant. This phenomenon, in which GO was partly reduced in the reaction, was also found in reports when GO was used as a carbocatalyst in catalytic oxidation of benzyl alcohol¹⁵ and the oxidative coupling of amines to imines.³⁹ The catalyst used after 10 cycles (N₂ atmosphere) was separated from the reaction solution and characterized by XRD, XPS, SEM, and TEM. Compared with the fresh GO, XRD (Figure S1, Supporting Information) of the GO used for 10 cycles shows a pattern similar to that of the starting GO, indicating this material was stable in the reaction and not aggregated. The morphology of the used GO in the reaction exhibited no noticeable difference under SEM and TEM observations, as shown in Figure S2. HRTEM shows that both the fresh GO and used GO exhibited the typical nanosheet structure of graphene consisting of 1–10 graphene layers.

From the XPS and Raman analysis (Figure S3, Figure S4, Table S2), the used GO in the oxidation reaction did not show any obvious difference from starting GO materials, such as the oxygen signal intensity and the C/O ratio or the ratio of the I_D/I_G in Raman spectrum. To understand how GO functioned as a direct oxidant, the states of O in the materials were investigated by C 1s XPS. The deconvoluted C 1s XPS core levels of fresh GO and used GO in N₂ atmosphere for 10 cycles are shown in Figure 2. The O contents assigned to C–O/C–O–C, C=O, and HO–C=O from Figure 2 were calculated and are shown in Table 2. The deconvoluted peak located at the binding

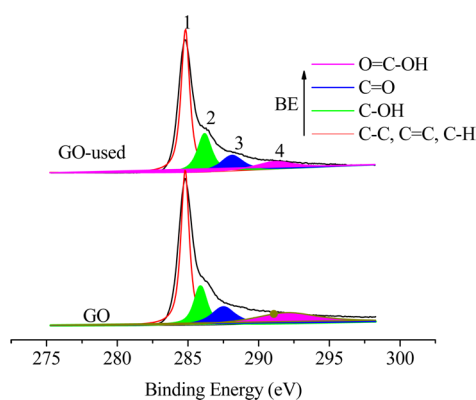


Figure 2. C 1s peak in the XPS spectra of fresh GO (down) and GO used for 10 cycles. The curve was fitted considering the following contributions: C–C, C=C, C–H (peak 1), C–O/C–O–C (hydroxyl and epoxy groups; peak 2), C=O (carbonyl groups; peak 3), and O=C–OH (carboxyl groups; peak 4).

Table 2. Distribution of Oxygen Species from the Deconvolution of C 1s by XPS

samples	total O/C at. %	(C–O) O ₁ /C at. %	(C=O) O ₂ /C at. %	(O=C–OH) O ₃ /C at. %
fresh GO	21.90	6.54	5.85	9.51
used GO in N ₂	20.58	9.43	6.04	5.11

energy of ~285.0 eV was attributed to the C–C, C=C, and C–H bonds. The deconvoluted peak centered at the binding energies of ~286.0, 287.5, and 289.5 were assigned to the C–OH, C=O, and O=C–OH oxygen-containing carbonaceous bands, respectively.⁴⁰ The spectra in Figure 2 indicate that the oxygen content in the form of carboxylic acid groups decreased, and the content in the form of carbonyl groups, hydroxyl, or epoxy increased. These results suggest that the GO catalyst underwent partial reduction during the conversion of HMF into DFF and afforded a carbon product that was similar to the rGO's and CMGs that have been previously reduced by a low-concentration sodium borohydride solution.¹⁸ Sergio Navalon et al.⁴¹ also indicate that GO materials are labile, as compared with graphene or doped graphene with heteroatoms. In the presence of a reducing reagent, the material can experience significant chemical changes in the nature of the functional groups.

To determine whether the oxygen molecule can be activated and participate in the oxidation of HMF, the aforementioned oxidation reaction was performed under 0.4 MPa of oxygen pressure. After 3 h at 100 °C, a HMF conversion of 91.9% with DFF selectivity up to 98.5% was reached (Table 1, entry 12). Continued heating of this reaction mixture under 0.4 MPa oxygen pressure afforded 98.1% HMF conversion for another 3 h. These controlled experiments (Table 1, entries 10, 11, 12) indicate that the oxygen molecule was activated by the GO material and participated in the oxidation reaction. More impressively, the GO catalyst showed good recyclability and can be reused by simple filtration and rinsing in acetonitrile. There were just slight decreases in both the relative activity and DFF selectivity (Figure 3) during up to eight cycles. The reactivity decrease in the aerobic catalytic oxidation can be attributed to the continued reduction of the oxygen groups in

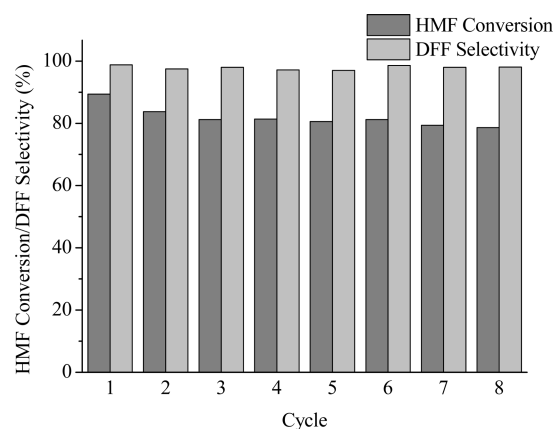


Figure 3. Recyclability of GO in aerobic oxidation of HMF. Conditions: HMF, 1 mmol, 126 mg; acetonitrile, 30 mL; TEMPO, 1 mmol, 155 mg; GO, 100 mg; reaction temperature, 100 °C; reaction time, 12 h; stirring speed, 800 rpm; 1 atm air pressure in 100 mL autoclave.

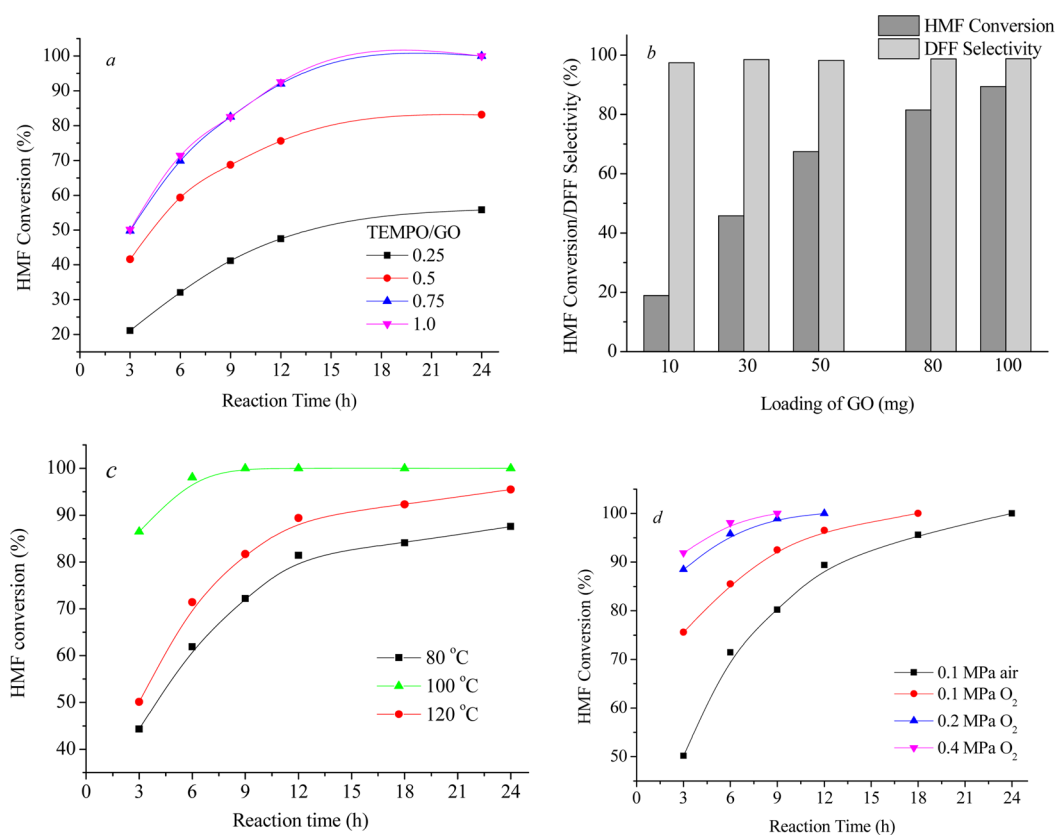


Figure 4. Catalytic behavior of GO on aerobic oxidation of HMF into DFF under different conditions. (a) Conversion of HMF versus mass ratio of TEMPO to GO. HMF, 1 mmol, 126 mg; acetonitrile, 30 mL; reaction temperature, 100 °C; 1 atm air pressure in 100 mL autoclave, stirring speed, 800 rpm. (b) Effect of the GO loading on HMF conversion. HMF, 1 mmol, 126 mg; acetonitrile, 30 mL; TEMPO, 1 mmol, 155 mg; reaction time, 12 h; stirring speed, 800 rpm; 1 atm air pressure in 100 mL autoclave. (c) Effect of reaction temperature on HMF conversion. HMF, 1 mmol, 126 mg; acetonitrile, 30 mL; TEMPO, 1 mmol, 155 mg; GO, 100 mg; stirring speed, 800 rpm. (d) Effect of oxygen pressure on HMF conversion. HMF, 1 mmol, 126 mg; acetonitrile, 30 mL; TEMPO, 1 mmol, 155 mg; GO, 100 mg; stirring speed, 800 rpm.

GO. Sequentially, the loss of oxygen groups in GO induced the loss of the ability of GO to act as a direct oxidant and carbocatalyst.

Above all, the performance of the GO/TEMPO system in catalytic oxidation of HMF into DFF is comparable or even superior to that of metal catalysts.^{1,14,42} Ultrasonic exfoliated GO (XPS in Figure S5 shows most oxygen groups were retained in GO) was also applied in this catalytic reaction; however, the results were negative. Under the same aforementioned reaction conditions, a HMF conversion of 13.1% was observed (Table 1, entry 15). This result can be attributed to the difficulty of HMF molecule accessing the active sites on GO. After the ultrasonic exfoliated GO was treated with NaOH and HCl aqueous solution according to the literature,³⁹ the HMF conversion significantly reached 35.6% (Table 1, entry 16). The base and acid treatment can increase the density of nanovoids in GO and then give rise to a high density of edges that have localized spins.³⁹ In addition, by removal of most hydroxyl and epoxide groups on GO basal plane with base and acid treatment, the catalytic sites of GO were more accessible to the reactant. The catalytic results in Table 1 suggest that thermal exfoliating of graphite oxide under a vacuum has a similar effect in conferring GO material the catalytic oxidation ability by removal of most hydroxyl and epoxide groups (in the forms of CO and CO₂) accompanied by creation of nanovoids in the GO materials (XPS in Figure 2 and SEM in Figure S2).

Aerobic Oxidation of HMF into DFF under Different Conditions. The reaction behavior of aerobic oxidation of HMF to DFF in the GO/TEMPO catalytic system under different conditions was investigated.

Control experiments show that the catalytic reaction without TEMPO gave a low HMF conversion (Table 1, entry 1). The effect of the TEMPO concentration on the HMF conversion was investigated (Figure 4a). Under all investigated reaction times, HMF conversion increased with an increasing TEMPO-to-GO mass ratio. When the mass ratio of TEMPO to GO was above 0.75, the increase started to level out, and further addition of TEMPO led to unnoticeable increases in HMF conversion at the same reaction time. To exclude the impact of TEMPO concentration on the HMF conversion, an excess amount of 1 M mol quantity of TEMPO was used in the following catalytic tests.

The effect of catalyst loading, reaction temperature, and oxygen pressure on HMF conversion were also investigated and are shown in Figure 4b–d. The results show that, as expected, HMF conversion increased with an increase in the amount of catalyst, reaction temperature, and oxygen pressure. Importantly, the selectivity to DFF remained at a relatively constant and high level (>95%, not shown in Figure 4a,c,d) while the conditions were varied. This result suggests that the GO–TEMPO catalytic system has a unique advantage in aerobic oxidation of HMF to DFF. A problem that should be noted is that high loading of GO was employed to ensure a good HMF

conversion (up to 80 wt %), which was also noted in early reports.^{15,24} The morphology and functionalities of GO need to be engineered using an effective method to improve its efficiency.

Catalytic Behavior of Thermally Annealed GOs under Different Temperatures. The above results have shown that carboxylic acid groups in GO were partially reduced into a carbonyl group, hydroxyl, or epoxy in anaerobic oxidation of HMF. The GO materials still own the ability to activate molecular oxygen during aerobic oxidation. Su and Loh²⁴ also indicated that because of the myriad oxygen atoms, GO can function as an oxidant during anaerobic oxidation and become reduced at the end of the first catalytic cycle. After that, the partially reduced GO can continue activating molecular oxygen during aerobic oxidation. Importantly, the real catalyst should be the partly reduced GO (rGO), rather than GO itself.²⁴ We suggest that GO can function as an oxidant and carbocatalyst simultaneously in aerobic oxidation of HMF into DFF. To determine which component in GO was responsible for the aerobic catalytic oxidation of HMF, the exfoliated GO was thermally reduced under a flowing He atmosphere at different temperatures in a tube furnace for 3 h. On the basis of the temperatures at which the GO's were thermal reduced, they were denoted as GO-T (T stands for the temperature of the treatment at 400, 700, 1000, and 1000-H, 1000-H stands for the highly reduced GO at 1000 °C for 10 h). After the GO was thermal reduced, the BET surface area and average pore diameter did not show obvious differences compared with the starting material (Table S3).

The thermal gravimetric analysis (TGA) of GO under argon flow with a heating rate of 5 °C/min is shown in Figure 5. The

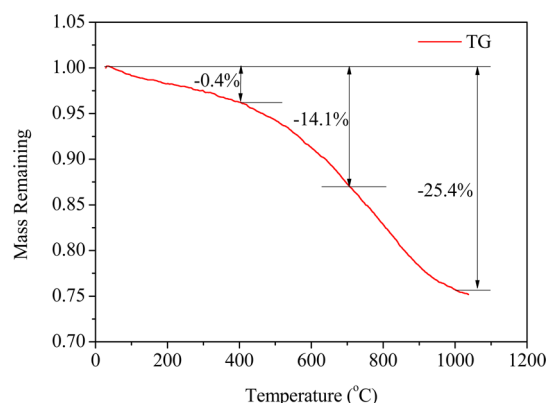


Figure 5. Thermal analysis of GO powder. Ar flowing rate, 30 mL/min; heating rate, 5 °C/min. TGA shows 25.4% mass loss at a temperature of 1000 °C for this particular run.

curve shows a continued mass loss during the increasing temperature. The weight losses under different temperature intervals are marked on the figure, and the overall weight loss was 25.4% while the temperature increased to 1000 °C. Mass spectrometry analysis showed that the components in the released gas were water, CO, and CO₂. The gradual weight loss can be attributed to the loss of residual oxygen functional groups in GO. This phenomenon shows that GO can be reduced to different levels by controlling the treatment temperatures and time.

In Figure 6, XRD of thermally annealed GO samples under different temperatures are also shown. The GO samples show two well-resolved reflections at 8.6° ($d = 1.02$ nm) and 28.8° (d

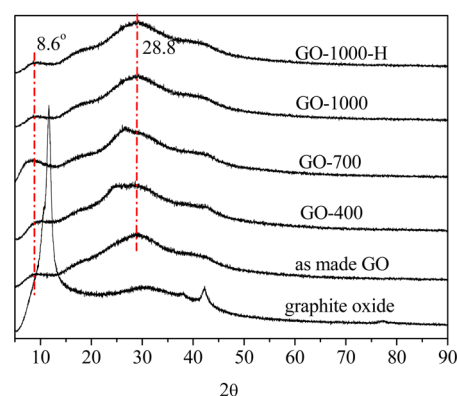


Figure 6. XRD patterns of thermal exfoliated GO and GO-T.

= 0.32 nm). The average interlayer distance was ~0.32–0.34 nm, closer to the interlayer distance of graphite (~0.34 nm), as a result of the thermal expansion and removal of oxygen functional groups. The morphology of the GO-T (Figure S6a,b,c,d) was determined by TEM and SEM methods. TEM and SEM of GO and GO-T show randomly aggregated, crumpled sheets, and no obvious differences were exhibited. HRTEM characterization further indicates that these nano-sheets consist of 1–10 layers of graphene.

Figure 7 shows the XPS signal intensity of O species in GO and GO-T. XPS revealed that thermal treatment induced a

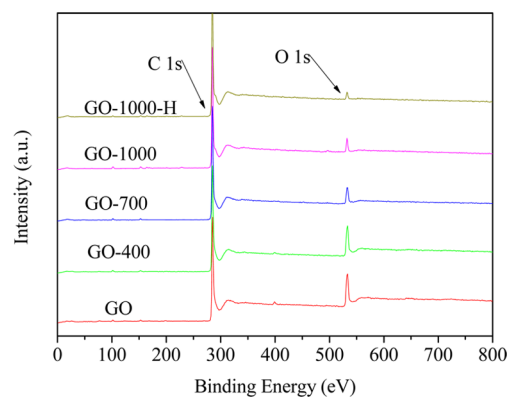


Figure 7. XPS patterns of the GO and GO-T samples.

continued decrease in the O content with an increase in the treatment temperature. Element analysis indicates that the C/O ratio in GO increased from 4.68 to 6.82, 13.47, 20.64, and 40.36, respectively, for GO-400, GO-700, GO-1000, and GO-1000-H (Table S2, Supporting Information). Figure 8 compares the Raman spectra of GO and GO-T samples. All samples display two intense bands. The D band (~1350 cm⁻¹), which as a breathing mode of k -point phonons of A_{1g} symmetry, is attributed to local defects and disorders, particularly the defects located at the edges of graphene and graphite platelets. The G band (~1580 cm⁻¹) is generally assigned to the E_{2g} phonon of the sp² bond of carbon atoms.⁴⁰ The larger I_D/I_G peak intensity ratio of a Raman spectrum can indicate higher defects and disorders of the graphitized structures containing the disorders caused at the edges of the carbon platelets. In addition, the intensity ratio of the 2D band to the D + G band located at ~2700–3000 cm⁻¹ can also be an indicator to judge the recovery of graphitic electronic conjugation.⁴³ In Figure 7, the D and G bands are displayed

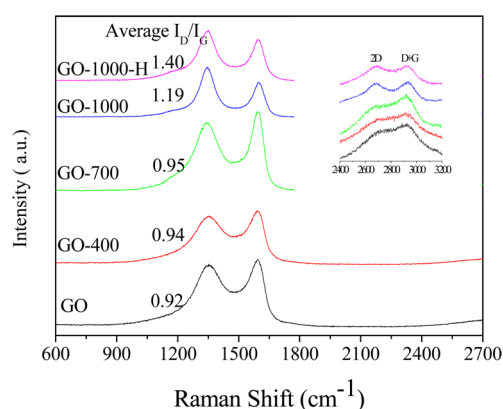


Figure 8. Visible Raman spectra of the GO and GO-T samples.

at about 1345 and 1592 cm^{-1} . The I_D/I_G ratio increased from 0.93 for the GO to 1.40 for GO-1000-H. The I_{2D}/I_{2G} ratio also increased from 0.91 for GO to 1.01 for GO-1000-H (Table S2). This increase was assigned to the removal of oxygen functionalities and formation of the pores (as defects and disorders) in the graphene sheets. These results clearly show that GO was reduced efficiently to different levels by controlling the treatment temperature.

Aerobic oxidation of HMF in the GO-T/TEMPO catalytic system was examined, and the results are shown in Figure 9.

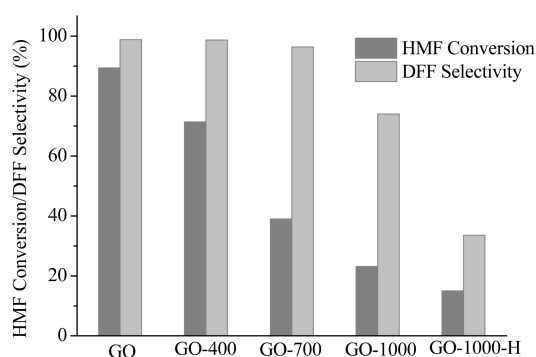


Figure 9. Aerobic oxidation of HMF in the GO-T/TEMPO catalytic system. Reaction conditions: HMF, 1 mmol, 126 mg; acetonitrile, 30 mL; GO-T, 100 mg; TEMPO, 1 mmol, 155 mg; reaction temperature, 100 °C; reaction time, 12 h; 1 atm air pressure in 100 mL autoclave; stirring speed, 800 rpm.

The reaction activity decreased with an increase in the GO treatment temperature. Significantly, for the GO samples treated above 700 °C in He, a drastic loss in the reaction activity were observed. In addition, the selectivity to DFF shows a decrease at some degrees compared with GO and GO-400. When the GO sample was treated at 1000 °C for 10 h (GO-1000-H), the HMF conversion and DFF selectivity were

reduced to 15.1% and 33.6% respectively, indicating the GO-1000-H almost lost its catalytic activity (compared with the result in Table 1, entry 2). However, the catalytic contribution from GO defects, including reactive edges, corners, and carbene cannot be excluded completely for the conversion of HMF into DFF.^{24,41}

It has been demonstrated that manganese in the active state (Mn_3O_4) owns the catalytic ability in aerobic oxidation of HMF.¹¹ Mn-based impurities in graphene were also demonstrated to be a key factor that had a crucial effect on the oxygen reduction reaction.⁴⁴ On the basis of elemental analysis and ICP results, we notice that the GO-T materials contained an impurity of manganese. As shown in Table S4, GO-T materials contained around 240–270 ppm Mn, and the contents of Mn in all the GO samples were relatively constant and independent of the thermal treatment temperature. However, the oxygen contents by elemental analysis show a monotonic decrease from 18.64 to 4.37 wt % with an increase in the treatment temperature. The constant Mn content and significant decrease of HMF conversion indicate that the active sites in GO should be oxygen species, rather than a Mn component.

To check whether the Mn component remained in the GO material was crucial for the GO catalytic activity in the HMF aerobic oxidation. The GO material was washed by a HCl aqueous solution,³⁹ and the Mn concentration in the GO decreased to ~45 ppm. The following catalytic test showed that the HMF conversion was independent of the amount of Mn in the GO (Table S4, entries 1, 6). In addition, three Mn/GO-1000-H samples were prepared by an impregnation method with their Mn concentrations up to 2700, 5400, and 8100 ppm, where the Mn concentrations in Mn/GO-1000-H were 10, 20, and 30 times that in pristine GO-1000-H. Catalytic tests showed no obvious change in the HMF conversion (Table S4, entries 7–9). The above results imply that the activity of the GO did not originate from Mn and was not affected by the Mn content.

To better understand the catalytic reaction, the bonding configurations and the number of oxygen atoms in GO-T were investigated by high-resolution C 1s XPS (Figure S7 and Table 3). As shown in Figure S7, the C 1s peaks in the high-resolution XPS spectra of these GO materials can be fitted into four peaks. The peak located at a binding energy of 285.0 eV was attributed to the C–C, C=C, and C–H bonds. The deconvoluted peaks centered at ~285.0, 286.0, 287.5, and 289.5 eV were assigned to the C–OH, C=O, and O=C–OH oxygen-containing carbonaceous bands, respectively.⁴⁰ The atomic contents of C and O elements in these samples calculated from XPS spectra were summarized in Table 3. It can be seen from Table 3 that the O atomic content decreased monotonically from 12.79 to 2.42 at. % with the increase in the treatment temperature from 400 to 1000 °C, which is consistent with elemental analysis results. Under the same reaction conditions, HMF conversion

Table 3. Distribution of Element Species in GO Samples Obtained from the Deconvolution of the C 1s Peaks by XPS

entry	binding energy(eV)	at. %				
		GO	GO-400	GO-700	GO-1000	GO-1000-H
total carbon (C)		82.12	87.21	93.04	95.37	97.58
total oxygen (O)		17.88	12.79	6.96	4.63	2.42
oxygen of C–O	~286.0	5.37	3.62	2.57	0.93	0.84
oxygen of C=O	~287.5	4.80	3.50	1.52	1.76	0.55
oxygen of O=C–OH	~289.5	7.81	5.67	2.87	1.95	1.03

decreased continuously when the GO treatment temperature increased from 400 to 1000 °C (Figure 9).

Acidimetric titration is an effective method to determine the surface oxides on a carbon or graphene oxide.^{45–47} The acidity of given functional groups depend on their chemical environment, that is, the size and shape of the polyaromatic layers, the presence and position of other substituents, and the charge of neighboring dissociated groups. However, the differences in acidity of the various types of functional groups seem to be sufficiently large to allow differentiation by a simple titration method.⁴⁶ These groups differ in their acidities and can be differentiated by neutralization with 0.05 N solutions of NaHCO₃, Na₂CO₃, NaOH, and NaOC₂H₅. In a simple way, the GO samples were agitated with an excess of the bases, and the excess base was determined by back-titration after equilibration (the detailed titration procedure is described in the Supporting Information). By titration, different oxygen groups in GO were calculated and are summarized in Table 4.

Table 4. Oxygen Groups in GO Samples Determined by Acidimetric Titration Techniques

samples	<i>n</i> (RCOOH) (mmol/g)	<i>n</i> (C=O) (mmol/g)	<i>n</i> (C–OH) (mmol/g)	<i>n</i> (COOCORe) (mmol/g)
GO	0.54	0.52	0.36	0.55
GO-400	0.40	0.47	0.34	0.23
GO-700	0.21	0.26	0.17	0.14
GO-1000	0.13	0.23	0.06	0.11
GO-1000-H	0.04	0.07	0.08	0.05

The results show that all oxygen groups decreased monotonically while the thermal treatment temperature increased, which is consisted with the above conclusion by XPS and elemental analysis.

Apart from the direct oxidation of HMF with carboxylic acid groups in GO were reduced to hydroxyl or epoxy groups, and molecular oxygen was activated and participated in the reaction. From the above catalytic oxidation results and characterization of the GO-T samples, it is unambiguous that the one or more oxygen functional groups in GO material have a crucial effect on the conversion of HMF to DFF. Which one (or more) is (are) the catalytic active species? According to the oxygen group concentrations in GO samples obtained from sodium uptake capacity results (Table 4), we plotted the initial reaction rate and total HMF conversion versus the oxygen functional group concentrations in GO samples during a specified reaction period. As shown in Figure 10, a good linear relationship was found between the carboxylic acid group concentration and the initial reaction rate and total HMF conversion. But for other oxygen functional groups, such as hydroxyl, carbonyl, or lactone group, no such good correlation can be established (Figure S8). This suggests that carboxylic acid groups were closely correlated with the conversion (anaerobic or aerobic) of HMF into DFF.

Probing the Origin of Catalytic Activity in GO. To confirm the catalytic oxygen groups in GO in HMF selective oxidation, various molecular analogues containing hydroxyl, carbonyl, anhydride, and carboxyl groups were tested as catalyst with TEMPO as the cocatalyst (Table 5).

As listed in Table 5, phenol, anhydride, and anthraquinone exhibited negligible HMF conversions in the selective oxidation of HMF (Table 5, entries 1–3). This result indicates that hydroxyl, anhydride, and carbonyl groups in GO could not

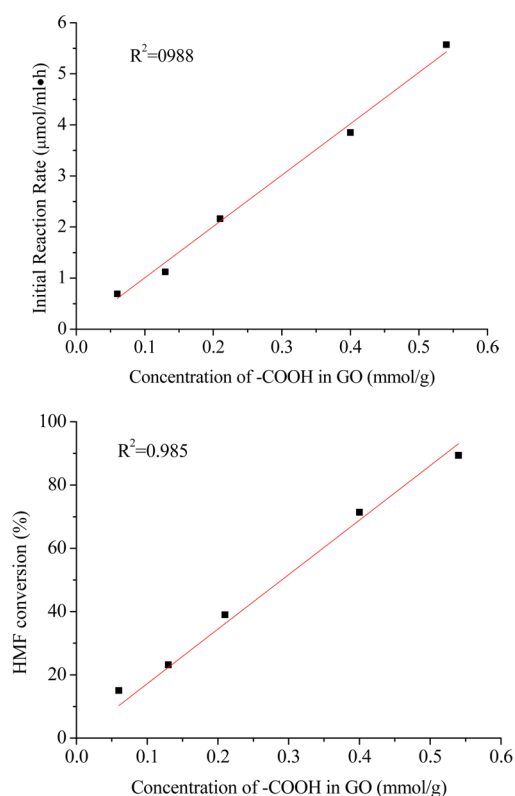
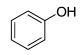
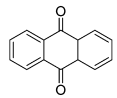
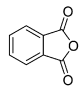
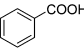
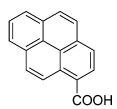
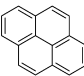
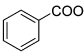
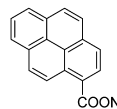
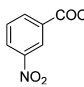
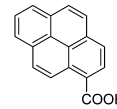
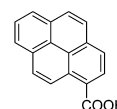


Figure 10. Relationship between initial reaction rate and total HMF conversion with carboxylic acid group concentration in GO samples.

constitute the catalytic site with TEMPO in the selective oxidation of HMF. When formic acid was used in this reaction system, 21.5% HMF conversion was observed; however, DFF selectivity was low (Table 5, entry 4). This implied that a degradation reaction of HMF occurred in which formic acid functioned as an acid catalyst. Acetic, hexanoic, benzoic, and 1-pyrene carboxylic acids have weaker acid strength than formic acid. In the catalytic tests, it was found that acetic, hexanoic, benzoic, or 1-pyrene carboxylic acid constituted an effective catalytic system with TEMPO in aerobic oxidation of HMF, and HMF conversions of 34.9, 35.2, 55.9, and 62.2%, respectively, were observed (Table 5, entries 5–8). It was also observed that pyrene itself had no activity in the aerobic oxidation of HMF (entry 10). Further experiments with sodium acetate, sodium benzoate, ethyl acetate, and sodium salt of 1-pyrene carboxylic acid showed that the catalytic behaviors were lost (entries 11–14), indicating the importance of hydrogen in the carboxylic acid groups. The activity of different carboxylic acids in the tested substrates increased in the following order: acetic acid ~ hexanoic acid < benzoic acid < 1-pyrene carboxylic acid \ll GO, and the site-time-yield (STY) increased from 6.9 to 15.5, 20.8, and 397.5 h⁻¹, respectively (Table 5, entries 5–9). This result demonstrates that the carboxylic acid–TEMPO system has the intrinsic activity in the aerobic oxidation of alcohols. Furthermore, the large π -conjugation system connected with carboxylic acid groups had a strong synergistic effect with the acid, giving an enhanced catalytic activity. 3-Nitrobenzoic acid was also tested, and the reactive activity decreased from 15.5 (benzoic acid) to 9.3 h⁻¹ (3-nitrobenzoic acid, Table 5, entry 15).

Studies show that GO or molecular analogues alone had a low catalytic ability in HMF oxidation (Table 1, entry 1; Table

Table 5. Control Experiments with Different Molecular Analogues As Catalyst^a

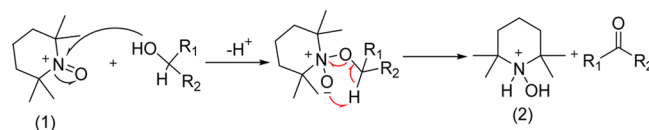
Entry	Tested Substrate	HMF Conv.%	DFF Selec.%	STY ^b ($\times 10^3$)
1		4.5	97.5	---
2		4.8	97.8	---
3		4.5	98.5	---
4	H-COOH	21.5	30.1	---
5	CH ₃ COOH	24.9	97.8	6.9
6	CH ₃ (CH ₂) ₄ COOH	27.0	97.1	7.5
7		55.9	97.7	15.5
8		75.2	99.5	20.9
9 ^c	GO	100	99.5	397.5
10		5.2	98.6	---
11	CH ₃ COONa	5.5	95.2	---
12		4.5	95.5	---
13		5.2	98.6	---
14	CH ₃ COOC ₂ H ₅	3.5	95.6	---
15		33.3	98.8	9.3
16 ^d		4.5	98.8	---
17 ^e		4.1	98.5	---

^aThe reactions were carried out with 0.3 mmol equiv of -COOH in molecular analogues and 1 M mol quantity of HMF, 155 mg of TEMPO dissolved in 30 mL CH₃CN; reaction temperature, 100 °C; stirring speed, 800 rpm; reaction time, 12 h; 0.4 MPa O₂ in 100 mL autoclave. ^bThe site-time-yield (STY) was calculated as the amount of HMF (mol) that converted into DFF per mol of -COOH in the catalyst per hour: (h⁻¹). ^c100 mg of GO was used in the reaction; reaction time, 3 h. The site-time-yield (STY) was calculated as the amount of HMF (mol) that converted into DFF catalyzed by GO per mol of -COOH in GO per hour (h⁻¹, excluding the contribution from GO as a direct oxidant). ^dWithout addition of TEMPO. ^eN₂ atmosphere in autoclave.

S, entry 16). Addition of TEMPO gave an obvious increase in the HMF conversion. Early reports have applied a ruthenium/TEMPO system to selective aerobic oxidation of alcohols to the corresponding aldehydes and ketones, in which TEMPO acted

as a hydrogen transfer mediator and was either regenerated by oxygen, under aerobic catalytic conditions, or converted to TEMPH under stoichiometric anaerobic conditions.⁴⁸

To determine whether TEMPO could function as an oxidant in the oxidation of HMF, the HMF oxidation reaction was performed in a 1-pyrene carboxylic acid-TEMPO system under an atmosphere of nitrogen (Table 5, entry 17). After 12 h and 100 °C, a 4.5% HMF conversion was achieved. This result demonstrates that TEMPO could not function as the oxidant in anaerobic oxidation of HMF. This control experiment also indicates that oxygen was important and should be the terminal oxidant. According to the literature,⁴⁸ in an oxidation system mediated by TEMPO and with a stoichiometric amount of a terminal oxidant (e.g., sodium hypochlorite, trichloroisocyanuric acid, *m*-chloroperbenzoic acid sodium bromite, sodium chlorite and oxone), the oxoammonium cation (Scheme 1) was generated and acted

Scheme 1. Oxidation Pathway of TEMPO-Mediated Oxidations

as the active oxidant (1). Alcohols transformed into corresponding aldehydes and ketones with the hydroxylamine (2), which was formed and reoxidized by the terminal oxidant to regenerate TEMPO.⁴⁸ We assume here that oxygen was critical in the formation of the oxoammonium cation and thus making the oxidation of HMF run smoothly.

According to the widely accepted Lerf-Klinowski model,³⁹ epoxy and hydroxyl groups resided on the GO basal plane, whereas the periphery of the GO sheets was decorated mainly by carboxyl, anhydride, lactone, phenol, lactol, or pyrone groups. Because the carboxylic acid groups were mainly residing at the periphery of the sheet, its coverage would be expected to be a relatively low proportion in GO (0.54 mmol/g of GO by acidimetric titration). It is difficult to explain the observed catalytic activity. SEM and TEM imaging has revealed that GO sheets expanded into 1–10 layers and became highly porous, with an average pore area around 14.3 nm in vacuum. Holes could be created during the harsh oxidation process, and the hole defects were enlarged during thermal exfoliating with partial oxygen groups that were removed in the form of CO and CO₂.⁴¹ These findings suggest that the active catalytic sites in GO are likely to be hole defects in the conjugated domain, and the edges of the hole defects were terminated by the carboxylic acid groups.

Electron spin resonance (ESR) measurements of GO materials are shown in Figure 11. The thermally reduced GO-T materials were also tested, and the ESR spectra are given in Figure S9 (Supporting Information). The ultrasonic exfoliated GO material gives only sharper peaks, with a line width close to that for sigma dangling bond spins in nanoporous carbon materials (~0.1 mT), corresponding to the previous report.³⁹ The thermally exfoliated GO (Figure 11) and thermally reduced GO-T materials (Figure S9) show the ESR peaks that have a line width similar to that of localized spins originating from the edge of nanographene (~1 mT), indicating the existence of unpaired spins originating from the edges of nanographene.^{39,49,50}

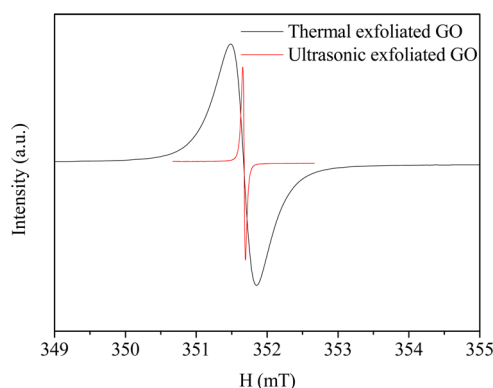


Figure 11. ESR measurement of GO materials exfoliated by different methods.

Thermal treatment of graphite oxide under vacuum conditions made graphite oxide exfoliated and partially reduced. Thermal exfoliating generates nanovoids that are surrounded by conjugated domains. Localized spins originating from the nonbonding π -electron states are likely to be created at the edges, analogous to nonkekule molecules having open shell unpaired electrons. The π -electron radical at the edges of graphene was delocalized along the edges to some extent and exhibits fast spin–lattice relaxation through interaction with the adjacent π -electron system, giving rise to a broad line width ~ 1

mT.³⁹ It has been proved that the synergistic effect of carboxylic acid groups and unpaired electrons at the edge defects impart to base–acid-processed GO material enhanced catalytic activity in aerobic oxidative coupling of amines to imines, in which base–acid-processed GO acted as the electron-transfer mediator.³⁹

In aerobic catalytic oxidation of HMF in the GO/TEMPO system, the TEMPO functioned as the active site in the form of oxoammonium cation by losing an electron, and an oxygen molecule was required for the formation of the oxoammonium cation. The GO material here would act as an electron transfer mediator from the TEMPO to oxygen. Therefore, it can be inferred that the enhanced catalytic activity of the thermally exfoliated GO in the GO/TEMPO system, compared with other molecular analogues in Table 5 and ultrasonically exfoliated GO (Table 1, entry 15), originated from the synergistic effect of carboxylic acid groups and unpaired electrons at the edge defects.

Proposed Reaction Pathway for Aerobic Oxidation of HMF in GO/TEMPO Catalytic System. A possible reaction pathway of aerobic oxidation of HMF into DFF with molecular oxygen as the terminal oxidant in the GO/TEMPO catalytic system is proposed and is shown in Figure 12. The edge sites with unpaired electrons and carboxylic acid groups constituted the active sites and afforded enhanced kinetics for the molecular TEMPO and oxygen trapping and activation by a sequence of electron transport. One plausible mechanism involving both the

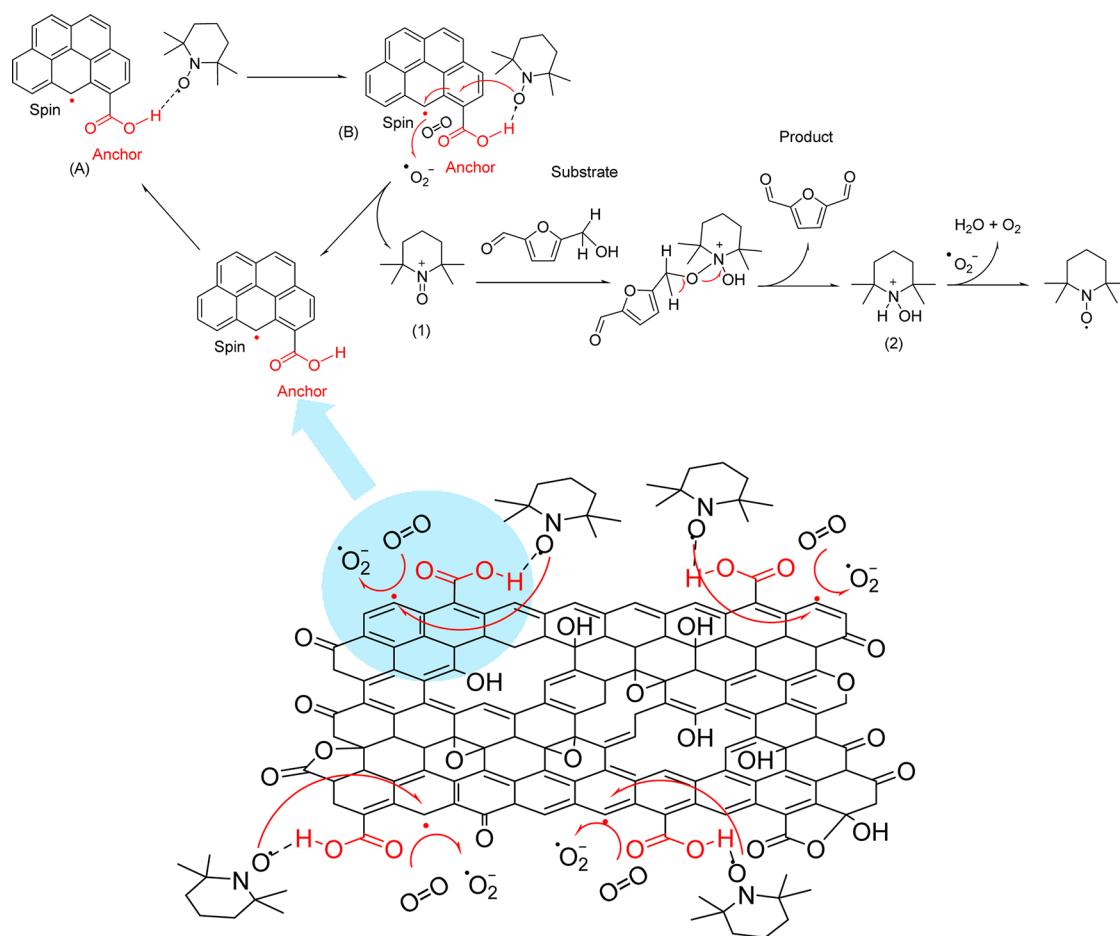


Figure 12. Proposed reaction pathway for selective oxidation of HMF to DFF with molecular oxygen as the terminal oxidant in the GO/TEMPO catalytic system.

unpaired electrons and the carboxylic acid groups is proposed as the following: TEMPO binds to the acidic carboxylic acid groups via a hydrogen bond (A) and forms an electron-donor complex (B). The unpaired electrons of porous GO reduce molecular oxygen to form $\bullet\text{O}_2^-$, which stays surface-bound to the GO to stabilize the positive charge of the holes. At the same time, the anchored TEMPO is oxidized by the positive charge of the hole to form the oxoammonium cation (1), and the active site on GO is regenerated. HMF is oxidized by the oxoammonium cation, producing DFF, and the produced hydroxylamine (2) is reoxidized by the superoxide radical. The TEMPO molecule is regenerated. Sequentially, the byproduct H_2O_2 decomposes into H_2O and oxygen under the reaction temperature.

CONCLUSIONS

In summary, the graphite oxide prepared from Hummers' method can be thermal exfoliated and partially reduced simultaneously under relatively mild condition. This procedure imparted high activities on GO in the anaerobic or aerobic oxidation of HMF into DFF in the presence of TEMPO. Nearly full HMF conversion and DFF selectivity can be obtained under optimized reaction conditions. The GO material can be used as a green oxidant. In addition, the carboxylic acid groups at the edges of the defects, along with the localized unpaired electrons, work synergistically to afford enhanced kinetics for the trapping and activation of molecular oxygen and TEMPO by a sequence of electron transport from TEMPO to molecular oxygen. The GO/TEMPO catalytic system facilitated the aerobic oxidation of HMF into DFF. With dwindling supplies of precious metals used for aerobic catalytic oxidation of HMF and other chemical syntheses, the prospect of replacing these metals with inexpensive carbon materials is extremely attractive and timely. It is envisaged that carbon-related materials, with an engineered morphology of functionalities, will emerge as powerful catalysts for mediating synthetic transformations.

ASSOCIATED CONTENT

Supporting Information

The Supporting Information is available free of charge on the ACS Publications website at DOI: 10.1021/acscatal.5b01446.

Synthesis of graphite oxide and thermally annealed GO in flowing He atmosphere. Experimental procedures. Analytic methods. Effect of solvents on HMF transformation. Plausible reaction pathway of GO as a direct oxidant in anaerobic oxidation of HMF to DFF catalyzed by TEMPO. Figures S1–10, Tables S1–5 (PDF)

AUTHOR INFORMATION

Corresponding Author

*Phone: +86 351 4049501. Fax: +86 351 4041153. E-mail: houxianglin@sxicc.ac.cn.

Notes

The authors declare no competing financial interest.

ACKNOWLEDGMENTS

This work was financially supported by the National Natural Science Foundation of China (NNSFC) (Grant 21403273), the National Key Basic Research Program of China (No. 2012CB215305), and Science Foundation of Shanxi Province (2013011010-6).

REFERENCES

- (1) Wang, Y.; Liu, B.; Huang, K.; Zhang, Z. *Ind. Eng. Chem. Res.* **2014**, *53*, 1313–1319.
- (2) Moreau, C.; Naceur Belgacem, M.; Gandini, A. *Top. Catal.* **2004**, *27*, 11–30.
- (3) Ma, J.; Du, Z.; Xu, J.; Chu, Q.; Pang, Y. *ChemSusChem* **2011**, *4*, 51–54.
- (4) Amarasekara, A. S.; Green, D.; McMillan, E. *Catal. Commun.* **2008**, *9*, 286–288.
- (5) Lichtenthaler, F. W. *Acc. Chem. Res.* **2002**, *35*, 728–737.
- (6) Shimo, T.; Ueda, S.; Suishu, T.; Somekawa, K. *J. Heterocycl. Chem.* **1995**, *32*, 727–730.
- (7) Antonyraj, C. A.; Jeong, J.; Kim, B.; Shin, S.; Kim, S.; Lee, K.-Y.; Cho, J. K. *J. Ind. Eng. Chem.* **2013**, *19*, 1056–1059.
- (8) Nie, J.; Xie, J.; Liu, H. *J. Catal.* **2013**, *301*, 83–91.
- (9) Hansen, T. S.; Sádaba, I.; García-Suárez, E. J.; Riisager, A. *Appl. Catal., A* **2013**, *456*, 44–50.
- (10) Le, N.-T.; Lakshmanan, P.; Cho, K.; Han, Y.; Kim, H. *Appl. Catal., A* **2013**, *464–465*, 305–312.
- (11) Liu, B.; Zhang, Z.; Lv, K.; Deng, K.; Duan, H. *Appl. Catal., A* **2014**, *472*, 64–71.
- (12) Liu, R.; Chen, J.; Chen, L.; Guo, Y.; Zhong, J. *ChemPlusChem* **2014**, *79*, 1448–1454.
- (13) Antonyraj, C. A.; Kim, B.; Kim, Y.; Shin, S.; Lee, K.-Y.; Kim, I.; Cho, J. K. *Catal. Commun.* **2014**, *57*, 64–68.
- (14) Sádaba, I.; Gorbanev, Y. Y.; Kegnaes, S.; Putluru, S. S. R.; Berg, R. W.; Riisager, A. *ChemCatChem* **2013**, *5*, 284–293.
- (15) Dreyer, D. R.; Jia, H.-P.; Bielawski, C. W. *Angew. Chem., Int. Ed.* **2010**, *49*, 6813–6816.
- (16) Fernández-Marino, M. J.; Guardia, L.; Paredes, J. I.; Villar-Rodil, S.; Solís-Fernández, P.; Martínez-Alonso, A.; Tascón, J. M. D. *J. Phys. Chem. C* **2010**, *114*, 6426–6432.
- (17) Li, X.; Wang, H.; Robinson, J. T.; Sanchez, H.; Diankov, G.; Dai, H. *J. Am. Chem. Soc.* **2009**, *131*, 15939–15944.
- (18) Shin, H.-J.; Kim, K. K.; Benayad, A.; Yoon, S.-M.; Park, H. K.; Jung, I.-S.; Jin, M. H.; Jeong, H.-K.; Kim, J. M.; Choi, J.-Y.; Lee, Y. H. *Adv. Funct. Mater.* **2009**, *19*, 1987–1992.
- (19) Stankovich, S.; Dikin, D. A.; Piner, R. D.; Kohlhaas, K. A.; Kleinhammes, A.; Jia, Y.; Wu, Y.; Nguyen, S. T.; Ruoff, R. S. *Carbon* **2007**, *45*, 1558–1565.
- (20) Zhao, J.; Pei, S.; Ren, W.; Gao, L.; Cheng, H.-M. *ACS Nano* **2010**, *4*, 5245–5252.
- (21) Becerril, H. A.; Mao, J.; Liu, Z.; Stoltenberg, R. M.; Bao, Z.; Chen, Y. *ACS Nano* **2008**, *2*, 463–470.
- (22) Zhu, Y.; Murali, S.; Cai, W.; Li, X.; Suk, J. W.; Potts, J. R.; Ruoff, R. S. *Adv. Mater.* **2010**, *22*, 3906–3924.
- (23) Pei, S.; Cheng, H.-M. *Carbon* **2012**, *50*, 3210–3228.
- (24) Su, C.; Loh, K. P. *Acc. Chem. Res.* **2013**, *46*, 2275–2285.
- (25) Scheuermann, G. M.; Rumi, L.; Steurer, P.; Bannwarth, W.; Mulhaupt, R. *J. Am. Chem. Soc.* **2009**, *131*, 8262–8270.
- (26) Nie, R.; Wang, J.; Wang, L.; Qin, Y.; Chen, P.; Hou, Z. *Carbon* **2012**, *50*, 586–596.
- (27) Wu, Z. S.; Yang, S.; Sun, Y.; Parvez, K.; Feng, X.; Mullen, K. J. *Am. Chem. Soc.* **2012**, *134*, 9082–9085.
- (28) Zhu, S.; Chen, C.; Xue, Y.; Wu, J.; Wang, J.; Fan, W. *ChemCatChem* **2014**, *6*, 3080–3083.
- (29) Dreyer, D. R.; Jia, H. P.; Todd, A. D.; Geng, J.; Bielawski, C. W. *Org. Biomol. Chem.* **2011**, *9*, 7292–7295.
- (30) Guo, S.; Sun, S. J. *Am. Chem. Soc.* **2012**, *134*, 2492–2495.
- (31) Jahan, M.; Bao, Q.; Loh, K. P. *J. Am. Chem. Soc.* **2012**, *134*, 6707–6713.
- (32) Li, Y.; Li, Y.; Zhu, E.; McLouth, T.; Chiu, C. Y.; Huang, X.; Huang, Y. *J. Am. Chem. Soc.* **2012**, *134*, 12326–12329.
- (33) Wang, S.; Zhang, L.; Xia, Z.; Roy, A.; Chang, D. W.; Baek, J. B.; Dai, L. *Angew. Chem., Int. Ed.* **2012**, *51*, 4209–4212.
- (34) Primo, A.; Neatu, F.; Florea, M.; Parvulescu, V.; Garcia, H. *Nat. Commun.* **2014**, *5*, 5291.
- (35) Watanabe, H.; Asano, S.; Fujita, S.-i.; Yoshida, H.; Arai, M. *ACS Catal.* **2015**, *5*, 2886–2894.

- (36) Long, J.; Xie, X.; Xu, J.; Gu, Q.; Chen, L.; Wang, X. *ACS Catal.* **2012**, *2*, 622–631.
- (37) Li, W.; Gao, Y.; Chen, W.; Tang, P.; Li, W.; Shi, Z.; Su, D.; Wang, J.; Ma, D. *ACS Catal.* **2014**, *4*, 1261–1266.
- (38) Duan, X.; O'Donnell, K.; Sun, H.; Wang, Y.; Wang, S. *Small* **2015**, *11*, 3036–3044.
- (39) Su, C.; Acik, M.; Takai, K.; Lu, J.; Hao, S. J.; Zheng, Y.; Wu, P.; Bao, Q.; Enoki, T.; Chabal, Y. J.; Loh, K. P. *Nat. Commun.* **2012**, *3*, 1298.
- (40) Akhavan, O. *ACS Nano* **2010**, *4*, 4174–4180.
- (41) Navalon, S.; Dhakshinamoorthy, A.; Alvaro, M.; Garcia, H. *Chem. Rev.* **2014**, *114*, 6179–6212.
- (42) Zhang, Z.; Yuan, Z.; Tang, D.; Ren, Y.; Lv, K.; Liu, B. *ChemSusChem* **2014**, *7*, 3496–3504.
- (43) Zhan, D.; Ni, Z.; Chen, W.; Sun, L.; Luo, Z.; Lai, L.; Yu, T.; Wee, A. T. S.; Shen, Z. *Carbon* **2011**, *49*, 1362–1366.
- (44) Wang, L.; Ambrosi, A.; Pumera, M. *Angew. Chem., Int. Ed.* **2013**, *52*, 13818–13821.
- (45) Boehm, H. P. *Angew. Chem., Int. Ed.* **2010**, *49*, 9332–9335.
- (46) Boehm, H. P. *Carbon* **2002**, *40*, 145–149.
- (47) Boehm, H. P. *Carbon* **1994**, *32*, 759–769.
- (48) Dijkstra, A.; Marino-González, A.; Mairata i Payeras, A.; Arends, I. W. C. E.; Sheldon, R. A. *J. Am. Chem. Soc.* **2001**, *123*, 6826–6833.
- (49) Enoki, T.; Takai, K. *Solid State Commun.* **2009**, *149*, 1144–1150.
- (50) Joly, V. L. J.; Takahara, K.; Takai, K.; Sugihara, K.; Enoki, T.; Koshino, M.; Tanaka, H. *Phys. Rev. B: Condens. Matter Mater. Phys.* **2010**, *81*, 115408.